Electronic Supplementary Material (ESI) for RSC Advances.

Supporting Information

Self-expansion, self-exfoliation and self-dispersion: insights into colloidal formation of atomically thin two-dimensional $MoO_{2.5}(OH)_{0.5}$

Hai Wang[ab*] and Yan Su[a]

[a]Key Laboratory of New Processing Technology for Nonferrous Metals and Materials, Ministry of Education, Guilin University of Technology, Guilin 541004, China

[b]Department of Electromechanical Engineering, Faculty of Science and Technology, University of Macau, Taipa, Macau

* To whom correspondence should be addressed.

Tel: +773-5896672. Fax: +773-5896671. E-mail: hbwanghai@gmail.com (H Wang).

Experimental section

Preparation of bulk MoO_3 nanobelts: All chemical reagents were commercial products used without further purification. Firstly, MoO_3 nanobelts were prepared via a facile hydrothermal approach, according to reported studies.[1] Typically, 1 g of ammonium molybdate was dissolved in 30 mL of deionized water under continuous stirring. After 30 min, 6 mL of HNO_3 was added to the beaker dropwisely and stirred for another 30 min. The homogeneous suspension was formed. Then the resulting suspension was transferred to a Teflon-lined autoclave with a capacity of 50 mL and then kept inside an electric oven at 180 °C for 24 h. The as-prepared MoO_3 nanobelts powder was collected by filtration and thoroughly washed with deionized water and ethanol for several times and finally dried in air. The single as-prepared MoO_3 nanobelts is consistent with our previously reported work, indicating single crystal structure.[2]

Preparation of bulk $MoO_{2.5}(OH)_{0.5}$ nanobelts: The two layer fibrous cloth (ca. 30.0mm×30.0 mm×0.5 mm) were placed on the top of Al_2O_3 crucible. 0.5 g of MoO_3 nanobelts powders were placed between two layer cloth. 20 mL of distilled water was poured into the crucible pool. Then all of them were transferred to a 50 mL Teflon-lined autoclave with 20 mL water, and then kept inside an electric oven at 180 °C for 24 h. The crucible with fibrous cloth was carefully taken out of the container. The powders were finally collected between the two layer cloth for further experiments and materials characterizations.

Preparation of monolayered $MoO_{2.5}(OH)_{0.5}$ sheets: The monolayered $MoO_{2.5}(OH)_{0.5}$ sheets were obtained by liquid exfoliating of as-prepared bulk $MoO_{2.5}(OH)_{0.5}$ nanosheets in water. In detail, 100 mg of bulk $MoO_{2.5}(OH)_{0.5}$ nanosheet powders dispersed in 100 mL water without any ultrasound for about 8 months.

Material characterizations: The crystal structure was performed by X-ray diffraction (XRD) analysis with a PANanalytic X'Pert spectrometer using Cu Kα radiation with wavelength of 0.15405 nm. The surface morphologies of the samples were studied using a JEOL JSM6300 (Tokyo, Japan) field emission scanning electron microscope (FESEM). The transmission electron microscopy (TEM) and high-resolution transmission electron microscopy (HRTEM) images were obtained with a JEM-2010F electron microscope (JEOL, Japan) operating at 200 kV. Atomic force microscopy (AFM) samples were prepared by drop drying the colloidal onto a mica substrate and the characterization was carried out on Veeco diInnova with a Si tip. UV-vis absorption spectra were recorded on a UV-4100 (Shimadzu) spectrometer between 200-800 nm. Photoluminescence spectra were collected by FLUOROLOG-3-TAU type spectrometer. The 330 nm exciting wavelength of a krypton ion laser (Coherent Innova) was used, with the nominal output power of the laser kept at 200 mW. All measurements were performed at room temperature. The zeta potential is an important and useful indicator of this charge that can be used to predict the stability of colloidal suspensions. The zeta potential of yellow colloidal particles was determined by a zeta potential analyzer (Zeta PALS, Brookhaven Instruments Co., USA).

Figure captions

Scheme. S1 The comparison of crystal structure of MoO_3 and $MoO_{2.5}(OH)_{0.5}$. Noted that the positions of the molybdenum atoms are different within the octahedra. The coordination of oxygen atoms (red spheres) around the molybdenum atoms (grey spheres) is respectively shown below MoO_3 and $MoO_{2.5}(OH)_{0.5}$.

Supplementary Note 1 The discussion of crystal structure of MoO_3 and $MoO_{2.5}(OH)_{0.5}$.

Fig. S1 The comparative XRD patterns of MoO_3 nanobelts under different conditions. Black: the MoO_3 nanobelts powders on the surface of Aluminum sheet; Red: the MoO_3 nanobelts powders on the surface of Nickel foam; Blue: the MoO_3 nanobelts powders on the surface of fibrous cloth at atmospheric conditions (room temperature and 1 atm).

Supplementary Note 2 The discussion of the formation mechanism of the obtained $MoO_{2.5}(OH)_{0.5}$.

Fig. S2 XPS spectras for Mo3d core level (a, b) and oxygen 1s level (c, d) of MoO_3 and $MoO_{2.5}(OH)_{0.5}$ nanobelts, respectively.

Fig. S3 FESEM image of the bulk MoO_3 nanobelts (a), the as-prepared $MoO_{2.5}(OH)_{0.5}$ nanobelts (b) and the residual unexfoliated $MoO_{2.5}(OH)_{0.5}$ nanobelts at the bottom of colloidal solutions (c).

Fig. S4 Photographs of the color changes of the $MoO_{2.5}(OH)_{0.5}$ nanosheets in water with increasing time.

Fig. S5 The TEM image of yellow colloidal solutions for ca 8 months.

Fig. S6 The TEM image of yellow colloidal solutions for ca 1 month.

Fig. S7 The TEM image of broken and tearing $MoO_{2.5}(OH)_{0.5}$ nanosheets.

Fig. S8 TEM image of single particle of yellow colloidal solutions for ca 8 months.

Fig. S9 (a) pristine $MoO_{2.5}(OH)_{0.5}$ colloidal solutions with low concentration; (b) $MoO_{2.5}(OH)_{0.5}$ suspension with addition of CTAB. After adding CTAB, the transparent solutions turned opaque, which clearly indicates that the $MoO_{2.5}(OH)_{0.5}$ colloidal solutions were negatively charged. The measured zeta potential value for pristine $MoO_{2.5}(OH)_{0.5}$ (a) is -28 mV(Fig. S10c) further confirmed that the $MoO_{2.5}(OH)_{0.5}$ colloidal solutions were negatively charged.

Fig. S10 Photographs of the $MoO_{2.5}(OH)_{0.5}$ nanosheets in various solvents of water, ethanol, NMP, formamide, IPA., respectively, after storage for 1 days at room temperature. It clearly demonstrates that water is promising solvent to exfoliate and disperse bulk $MoO_{2.5}(OH)_{0.5}$ nanosheets.

Supplementary Note 3 The discussion of why the resultant colloidal solutions are charged negatively and the origin of extra drive force of water molecular insertion into between the layers of $MoO_{2.5}(OH)_{0.5}$.

Table captions

Tab. S1. Comparison between our method and the previous exfoliation methods.

Tab. S2 Comparative results of the lattice parameters and unit cell volume between orthorhombic MoO_3 and orthorhombic $MoO_{2.5}(OH)_{0.5}$.

References

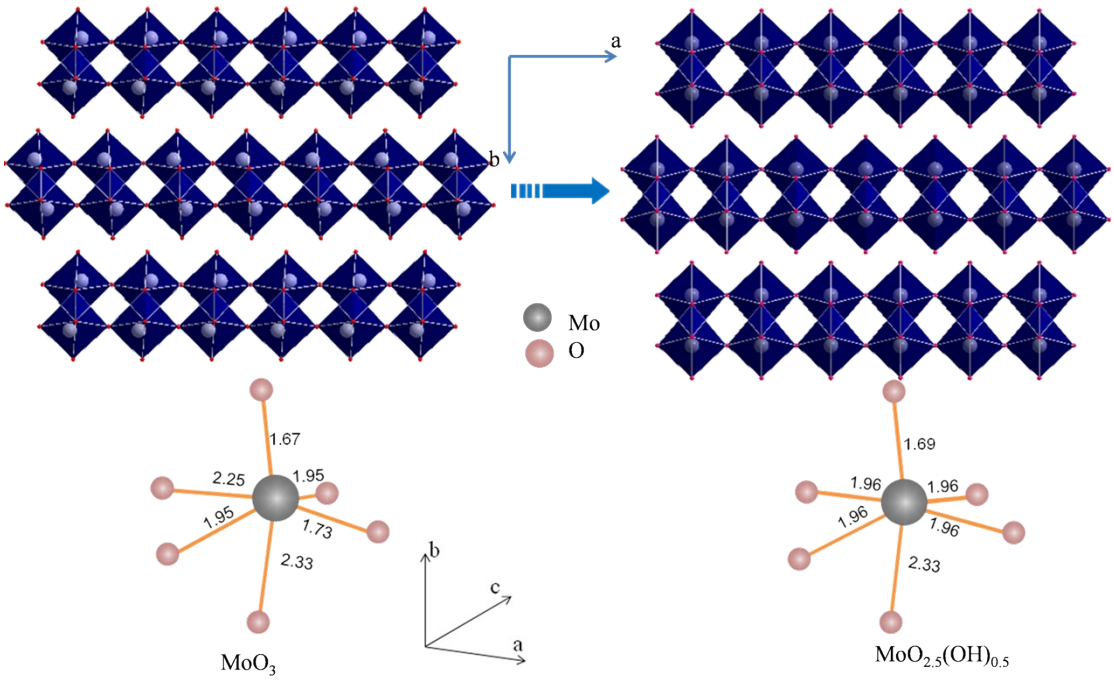

Scheme. S1. The comparison of crystal structure of MoO_3 and $MoO_{2.5}(OH)_{0.5}$. Noted that the positions of the molybdenum atoms are different within the octahedra. The coordination of oxygen atoms (red spheres) around the molybdenum atoms (grey spheres) is shown below MoO_3 and $MoO_{2.5}(OH)_{0.5}$, respectively.

Supplementary Note 1 | | The discussion of crystal structure of MoO_3 and $MoO_{2.5}(OH)_{0.5}$.

Based on the comparison of crystal structure of MoO_3 and $MoO_{2.5}(OH)_{0.5}$, the $MoO_{2.5}(OH)_{0.5}$ is remarkably similar to that of MoO_3. Two OH groups in $MoO_{2.5}(OH)_{0.5}$ substituted one O atom per unit cell of MoO_3.[3] When $MoO_{2.5}(OH)_{0.5}$ nanosheets were exfoliated into monolayered nanosheets, the MoO_6 monolayer in $MoO_{2.5}(OH)_{0.5}$ is also remarkably similar to that of MoO_3.

From a large number of exfoliated two-dimensional materials, such as graphene oxide and h-BN, in fact, a stable single-layer sheet is actually not a simple single-layer graphene and h-BN, but the "functionalized" single-layer graphite and single-layer h-BN, such as, graphene with OH groups, and h-BN with surface functionalization groups.[4-5] Therefore, for as-prepared single-layer $MoO_{2.5}(OH)_{0.5}$ in our work, it was considered as MoO_3 with "H" functionalization.

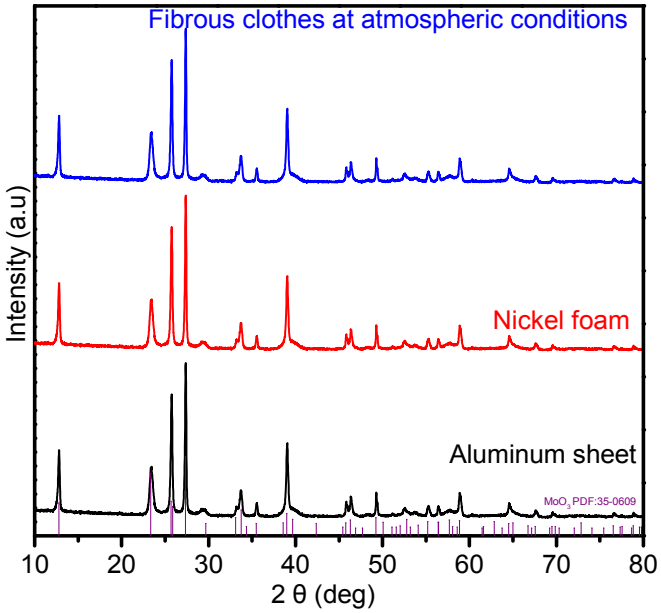

Fig. S1. The comparative XRD patterns of MoO_3 nanobelts under different conditions. Black: the MoO_3 nanobelts powders on the surface of Aluminum sheet; Red: the MoO_3 nanobelts powders on the surface of Nickel foam; Blue: the MoO_3 nanobelts powders on the surface of fibrous cloth at atmospheric conditions (room temperature and 1 atm).

Supplementary Note 2 | | The discussion of the formation mechanism of the obtained $MoO_{2.5}(OH)_{0.5}$.

Based on previously reported literature, $MoO_{2.5}(OH)_{0.5}$ was formed in a reducing environment.[3] Moreover, our XPS results further confirmed that Mo was a mixed valence state with +4 and +6. For our case, the fibrous cloth acted a double role during the formation of $MoO_{2.5}(OH)_{0.5}$, which may accelerate the decomposition of water vapor in high pressure. This may occur in the equation: $H_2O(g) + C(s) \rightarrow H_2(g) + CO(g)$.[6] The formation of H_2 is very favorable for the formation of $MoO_{2.5}(OH)_{0.5}$. In our previously reported literature, we also confirmed that carbon is a catalytic role in the formation of H_xMoO_3.[2]

Additionally, to validate the necessaries of fibrous cloth and "sauna reaction", we substituted fibrous cloth by other two different substrates, Aluminum sheet, Nickel foam. Compared to the proposed method, we found that the original MoO_3 powders were unchanged. Their corresponding XRD results also confirmed that the MoO_3 powders were not transformed into $MoO_{2.5}(OH)_{0.5}$. This evidence shows that fibrous cloth are necessary. Further, we also designed fibrous cloth at atmospheric conditions. The MoO_3 powders were placed between the two layer fibrous cloth. The color of MoO_3 powders were also unchanged under the action of the water vapor. Based on the results mentioned above, we reasonably inferred that both high pressure environment and fibrous cloth are necessary for the formation of $MoO_{2.5}(OH)_{0.5}$.

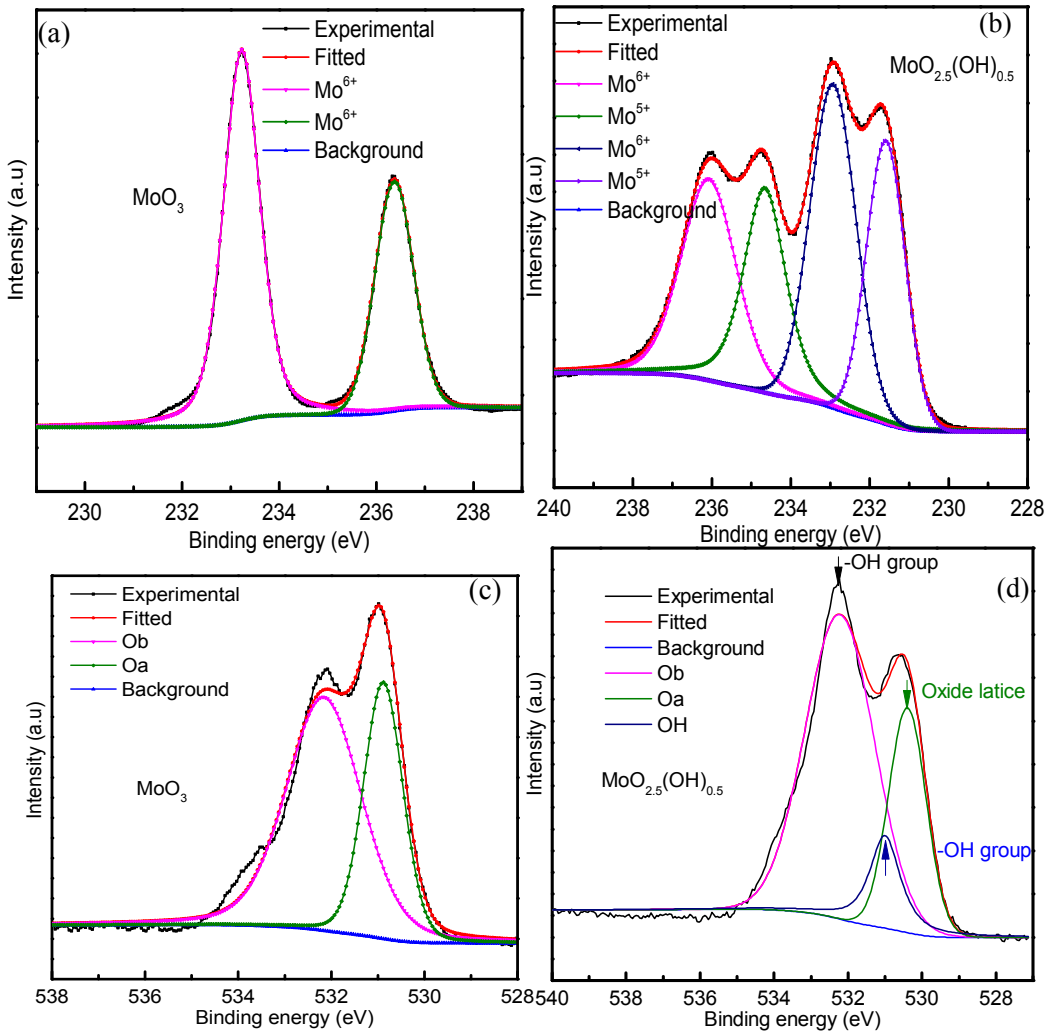

Fig. S2. XPS spectras for Mo3d core level (a, b) and oxygen 1s level (c, d) of MoO_3 and $MoO_{2.5}(OH)_{0.5}$ nanobelts, respectively.

The arrows indicate that both the highest peak at 532.23 eV and a weak peak at 531 eV in $MoO_{2.5}(OH)_{0.5}$ originated from the OH group.[7] Compared to MoO_3, the intensity of oxide lattice began to decrease, which may be the introduction of OH group. The effect of the break of oxygen bonds during "sauna reaction" may be a critical for hydrogen injection into the bulk MoO_3 nanobelts.[8]

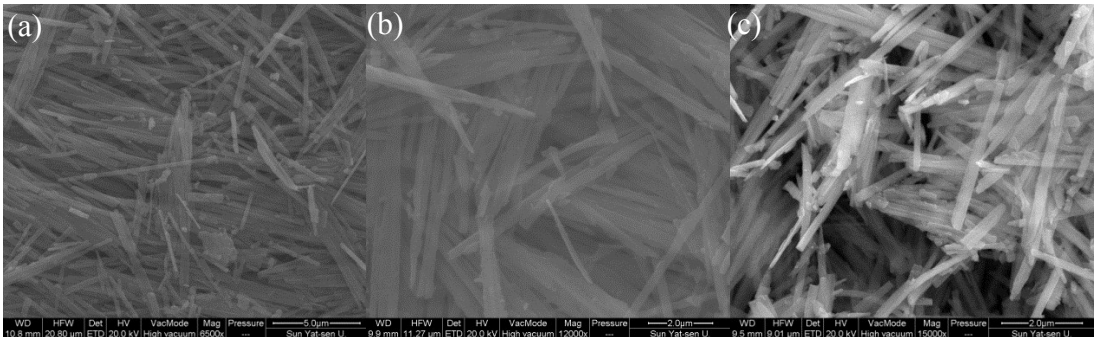

Fig. S3. FESEM image of the bulk MoO_3 nanobelts (a), the as-prepared $MoO_{2.5}(OH)_{0.5}$ nanobelts (b) and the residual unexfoliated $MoO_{2.5}(OH)_{0.5}$ nanobelts at the bottom of colloidal solutions (c).

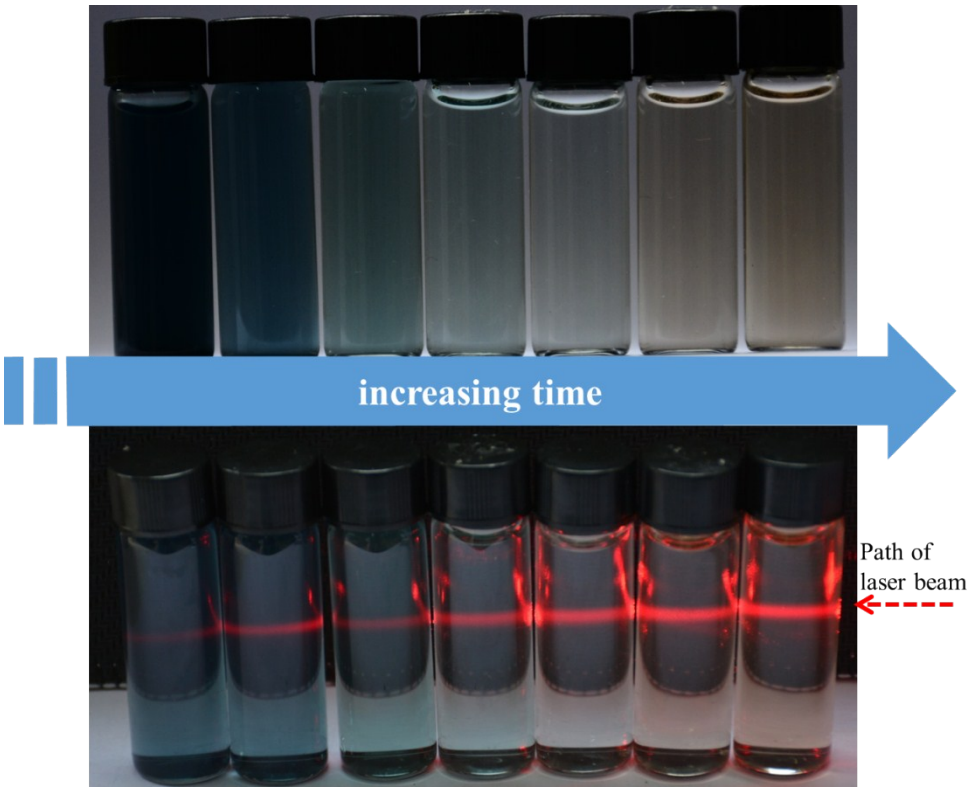

Fig. S4. Photographs of the color changes of the $MoO_{2.5}(OH)_{0.5}$ nanosheets in water with increasing time.

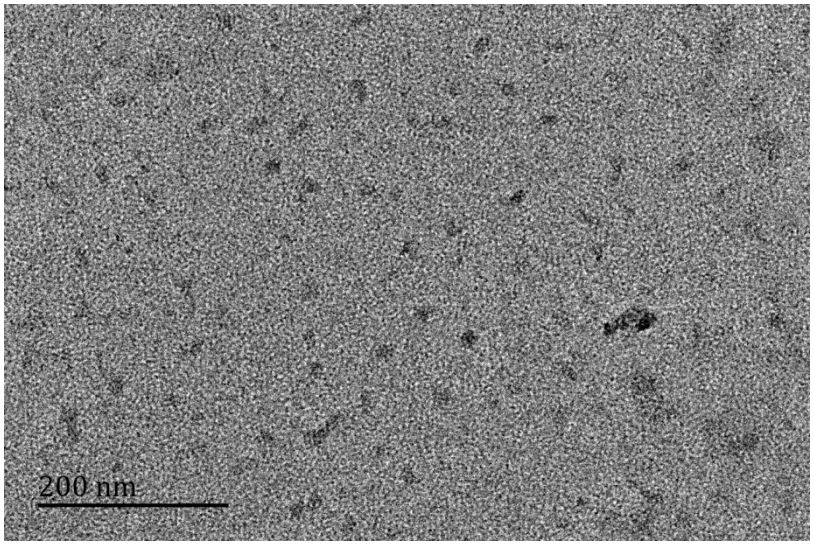

Fig. S5. The TEM image of yellow colloidal solutions for ca 8 months.

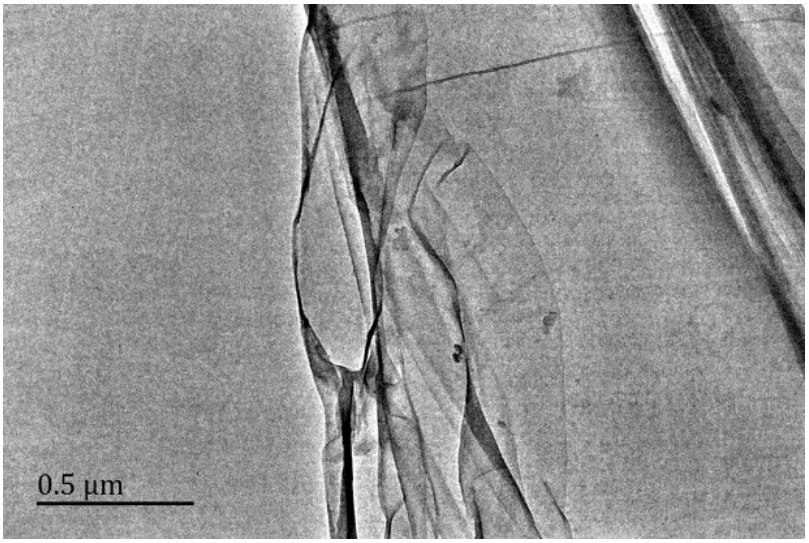

Fig. S6. The TEM image of yellow colloidal solutions for ca 1 month.

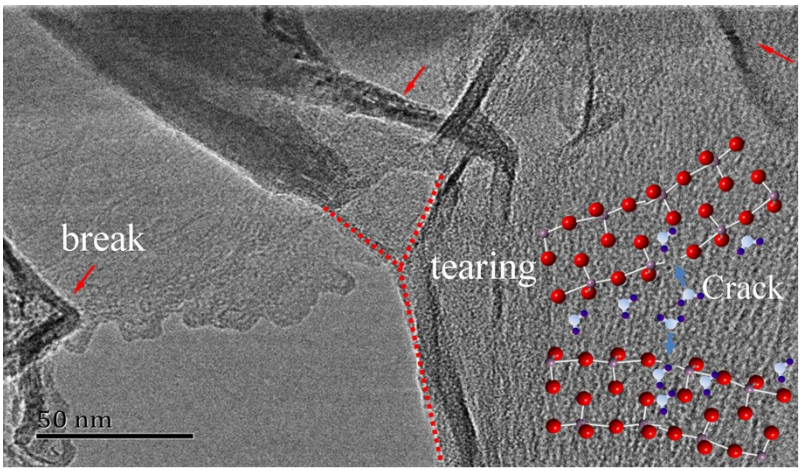

Fig. S7. The TEM image of broken and tearing $MoO_{2.5}(OH)_{0.5}$ nanosheets.

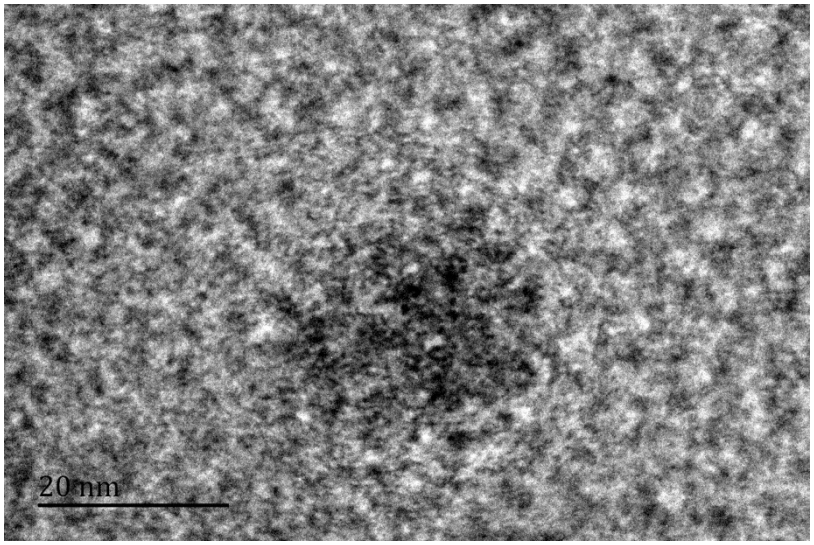

Fig. S8. TEM image of single particle of yellow colloidal solutions for ca 8 months.

It is curious that the crystalline lattice patter from TEM is unstable at high-energy electron beams at 200 keV. An electron beam can adversely affect an organic or inorganic sample during examination in a high-energy electron microscope, such as, 200 Kev. F. Egerton et al had discussed this issue of radiation damage in the TEM and SEM.[9] Similarly, Laruelle, S et al also found similar phenomina during the TEM observation.[10]

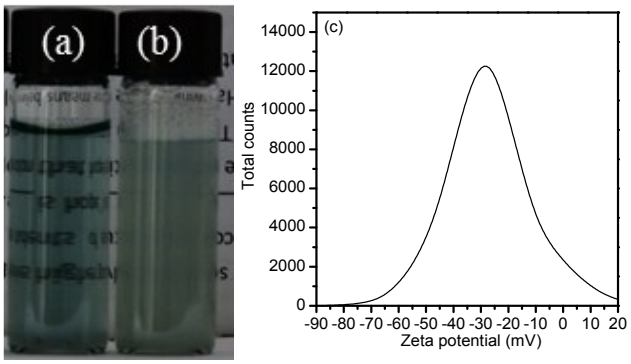

Fig. S9. (a) pristine $MoO_{2.5}(OH)_{0.5}$ colloidal solutions with low concentration; (b) $MoO_{2.5}(OH)_{0.5}$ suspension with addition of CTAB. After adding CTAB, the transparent solutions turned opaque, which clearly indicated that the $MoO_{2.5}(OH)_{0.5}$ colloidal solutions were negatively charged. The measured zeta potential value for pristine $MoO_{2.5}(OH)_{0.5}$ (a) was -28 mV(Fig. S10c) further confirmed that the $MoO_{2.5}(OH)_{0.5}$ colloidal solutions were negatively charged.

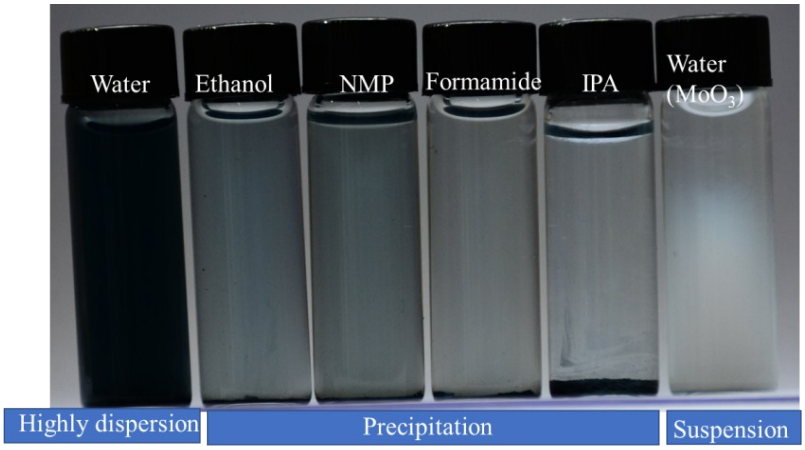

Fig. S10. Photographs of the $MoO_{2.5}(OH)_{0.5}$ nanosheets in various solvents of water, ethanol, NMP, formamide, IPA., respectively, after storage for 1 days at room temperature. It clearly demonstrates that water is promising solvent to exfoliate and disperse bulk $MoO_{2.5}(OH)_{0.5}$ nanosheets.

Tab. S1. **Comparison between our method and the previous exfoliation methods**

Colloidal solutions	Methods	functionalization	Reference
Few-layer boron nitride	one-step mechano-chemical process, complex	amino groups	[5]
Single-layered graphitic-C_3N_4	Three steps including acid treatment, $NH_3.H_2O$ treatment and ultrasonication, complex	unknown	[11]
	ultrasonication, complex	dangling hydrogens	[12]
Atomically thick g-C_3N_4-NSs	sulphuric acid, complex	oxygen functional groups	[13]
Exfoliated graphene-like carbon nitride	organic solvents, complex	dangling hydrogens	[14]
WS_2, MoS_2, $MoSe_2$, h-BN	Temperature assisted by ultrasonication, complex	edge functionalization	[15]
transition metal dichalcogenides	Cosolvent, complex	-CH_3 et al	[16]
graphene	intercalation, oxidation or functionalization, complex	-OH	[17-22]
MoS_2	solvent-assisted exfoliation via sonication, complex	unknown	[23]
MgB_2	solvent-assisted exfoliation via sonication, complex	-OH	[24]
Fewer layered MoS_2	Combined grinding and sonication	Unkown	[25]
	Solvent N-methyl-pyrrolidone and sonication, complex	Unknown, assisted by solvent	[26]
	Biocompatible block copolymers, complex	Unknown, assisted by biocompatible block copolymers	[27]
Graphene oxide nanosheets	Acoustic cavitation, complex	Unknown, assisted by K^+	[28]
$MoO_{2.5}(OH)_{0.5}$	Direct exfoliation and dispersion, simple	unnecessary	Our work

Tab. S2 Comparative results of the lattice parameters and unit cell volume between orthorhombic MoO_3 and orthorhombic $MoO_{2.5}(OH)_{0.5}$.

Sample phase	Symmetry	a (Å)	b (Å)	c (Å)	V (Å^3)	d_{020} (Å)
MoO_3	Orthorhombic 35-0609	3.963	13.856	3.6966	202.99	6.9212
$MoO_{2.5}(OH)_{0.5}$	Orthorhombic 14-0041	3.888	14.082	3.734	204.44	7.05

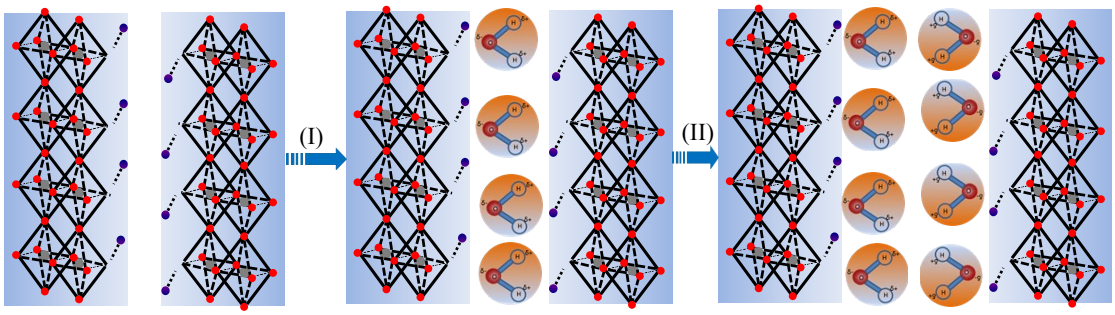

Scheme. S2. The schematic of the interaction of polar water molecular and negatively charged layer of $MoO_{2.5}(OH)_{0.5}$.

Supplementary Note 3 | | The discussion of why the resultant colloidal solutions are charged negatively and the origin of extra drive force of water molecular insertion into between the layers of $MoO_{2.5}(OH)_{0.5}$.

Before the final summary of the mechanism of colloidal formation of atomically thin two-dimensional $MoO_{2.5}(OH)_{0.5}$, we need to address two issues: (1) why are the resultant colloidal solutions charged negatively? (2) what is the origin of extra drive force of water molecular insertion into between the layers of $MoO_{2.5}(OH)_{0.5}$?

Based on analysis of XPS (Fig. S3), $MoO_{2.5}(OH)_{0.5}$ contained a mixture valence of Mo^{5+} and Mo^{6+}. Partially substitution of Mo^{5+} for Mo^{6+} in the octahedral sheet leads to negative charge, therefore, $MoO_{2.5}(OH)_{0.5}$ colloidal solutions are negatively charged. Polar water molecules can easily move into the space between negatively charged layers of $MoO_{2.5}(OH)_{0.5,}$ thus leading to its full expansion.

References:

(1) Phuruangrat, A.; Chen, J.; Lou, X.; Yayapao, O.; Thongtem, S.; Thongtem, T., Hydrothermal Synthesis and Electrochemical Properties of α-MoO_3 Nanobelts Used as Cathode Materials for Li-Ion Batteries. Appl. Phys. A **2012**, *107*, 249-254.

(2) Song, Y.; Wang, H.; Li, Z.; Ye, N.; Wang, L.; Liu, Y., H_xMoO_3@C nanobelts: Green Synthesis and Superior Lithium Storage Properties. International Journal of Hydrogen Energy **2015**, *40*, 3613-3623.

(3) Lars, K.; Göran, H.; Axel, R., On Molybdenum Oxide Hydroxides Genotypic with MoO_3. Acta. Chem. Scand **1961**, *15*, 1187-1188.

(4) Dreyer, D. R.; Park, S.; Bielawski, C. W.; Ruoff, R. S., The Chemistry of Graphene Oxide. Chemical Society Reviews **2010**, *39*, 228-240.

(5) Lei, W.; Mochalin, V. N.; Liu, D.; Qin, S.; Gogotsi, Y.; Chen, Y., Boron Nitride Colloidal Solutions, Ultralight Aerogels and Freestanding Membranes through One-Step Exfoliation and Functionalization. Nat. Commun. **2015**, *6*.

(6) W, S. T., Inorganic Chemistry. Academic Press: San Diego, **1997**.

(7) Lai, X.; Yan, M.; Liu, X.; Luo, J.; Tang, G.; Xie, F.; Chen, J.; Liu, P.; Di, S.; Xie, W.; Chen, Q., Investigation of Hydrogen Interaction with Pt-Coated Tungsten Oxide Hydrate Nanoplates. Mater. Res. Express **2014**, *1*, 025044.

(8) Xie, W.; Su, M.; Zheng, Z.; Wang, Y.; Gong, L.; Xie, F.; Zhang, W.; Luo, Z.; Luo, J.; Liu, P., Nanoscale Insights into the Hydrogenation Process of Layered α-MoO_3. ACS Nano **2015**, *10*, 1662-1670.

(9) Egerton, R. F.; Li, P.; Malac, M., Radiation Damage in the TEM and SEM. Micron **2004**, *35*, 399-409.

(10) Laruelle, S.; Grugeon, S.; Poizot, P.; Dollé, M.; Dupont, L.; Tarascon, J.-M., On the Origin of the Extra Electrochemical Capacity Displayed by MO/Li Cells at Low Potential. J. Electrochem. Soc **2002**, *149*, A627-A634

(11) Zhang, X.; Wang, H.; Wang, H.; Zhang, Q.; Xie, J.; Tian, Y.; Wang, J.; Xie, Y., Single−Layered Graphitic−C_3N_4 Quantum Dots for Two−Photon Fluorescence Imaging of Cellular Nucleus. Adv. Mater. **2014**, *26*, 4438-4443.

(12) Zhang, X.; Xie, X.; Wang, H.; Zhang, J.; Pan, B.; Xie, Y., Enhanced Photoresponsive Ultrathin Graphitic-Phase C_3N_4 Nanosheets for Bioimaging. J. Am. Chem. Soc. **2012**, *135*, 18-21.

(13) Zhao, F.; Cheng, H.; Hu, Y.; Song, L.; Zhang, Z.; Jiang, L.; Qu, L., Functionalized Graphitic Carbon Nitride for Metal-Free, Flexible and Rewritable Nonvolatile Memory Device via Direct Laser-Writing. Sci. Rep. **2014**, *4*.

(14) She, X.; Xu, H.; Xu, Y.; Yan, J.; Xia, J.; Xu, L.; Song, Y.; Jiang, Y.; Zhang, Q.; Li, H., Exfoliated Graphene-Like Carbon Nitride in Organic Solvents: Enhanced Photocatalytic Activity and Highly Selective and Sensitive Sensor for the Detection of Trace Amounts of Cu^{2+}. J. Mater. Chem. A **2014**, *2*, 2563-2570.

(15) Kim, J.; Kwon, S.; Cho, D.-H.; Kang, B.; Kwon, H.; Kim, Y.; Park, S. O.; Jung, G. Y.; Shin, E.; Kim, W.-G., Direct Exfoliation and Dispersion of Two-Dimensional Materials in Pure Water via Temperature Control. Nat. Commun. **2015**, *6*.

(16) Halim, U.; Zheng, C. R.; Chen, Y.; Lin, Z.; Jiang, S.; Cheng, R.; Huang, Y.; Duan, X., A Rational Design of Cosolvent Exfoliation of Layered Materials by Directly Probing Liquid-Solid Interaction. Nat. Commun. **2013**, *4*.

(17) Park, S.; Ruoff, R. S., Chemical Methods for the Production of Graphenes. Nat. Nanotech. **2009**, *4*, 217-224.

(18) Shih, C.-J.; Vijayaraghavan, A.; Krishnan, R.; Sharma, R.; Han, J.-H.; Ham, M.-H.; Jin, Z.; Lin, S.; Paulus, G. L.; Reuel, N. F., Bi-and Trilayer Graphene Solutions. Nat. Nanotech. **2011**, *6*, 439-445.

(19) Jin, Z.; Lomeda, J. R.; Price, B. K.; Lu, W.; Zhu, Y.; Tour, J. M., Mechanically Assisted Exfoliation and Functionalization of Thermally Converted Graphene Sheets. Chem. Mater. **2009**, *21*, 3045-3047.

(20) Li, D.; Mueller, M. B.; Gilje, S.; Kaner, R. B.; Wallace, G. G., Processable Aqueous Dispersions of Graphene Nanosheets. Nat. Nanotech. **2008**, *3*, 101-105.

(21) Stankovich, S.; Piner, R. D.; Nguyen, S. T.; Ruoff, R. S., Synthesis and Exfoliation of Isocyanate-Treated Graphene Oxide Nanoplatelets. Carbon **2006**, *44*, 3342-3347.

(22) Zeng, Z.; Yin, Z.; Huang, X.; Li, H.; He, Q.; Lu, G.; Boey, F.; Zhang, H., Single−Layer Semiconducting Nanosheets: High−Yield Preparation and Device Fabrication. Angew. Chem. Int. Ed. **2011**, *50*, 11093-11097.

(23) Jawaid, A.; Nepal, D.; Park, K.; Jespersen, M.; Qualley, A.; Mirau, P.; Drummy, L. F.; Vaia, R. A., Mechanism for Liquid Phase Exfoliation of MoS_2. Chem. Mater. **2015**, *28*, 337-348.

(24) Das, S. K.; Bedar, A.; Kannan, A.; Jasuja, K., Aqueous Dispersions of Few-Layer-Thick

Chemically Modified Magnesium Diboride Nanosheets by Ultrasonication Assisted Exfoliation. Sci. Rep. **2015**, *5*.

(25) Yao, Y.; Tolentino, L.; Yang, Z.; Song, X.; Zhang, W.; Chen, Y.; Wong, C. p., High−Concentration Aqueous Dispersions of MoS_2. Adv. Funct. Mater. **2013**, *23*, 3577-3583.

(26) O'Neill, A.; Khan, U.; Coleman, J. N., Preparation of High Concentration Dispersions of Exfoliated MoS_2 with Increased Flake Size. Chem. Mater. **2012**, *24*, 2414-2421.

(27) Mansukhani, N. D.; Guiney, L. M.; Kim, P. J.; Zhao, Y.; Alducin, D.; Ponce, A.; Larios, E.; Yacaman, M. J.; Hersam, M. C., High−Concentration Aqueous Dispersions of Nanoscale 2D Materials Using Nonionic, Biocompatible Block Copolymers. Small **2016**, *12*, 294-300.

(28) Han, J. T.; Jang, J. I.; Kim, H.; Hwang, J. Y.; Yoo, H. K.; Woo, J. S.; Choi, S.; Kim, H. Y.; Jeong, H. J.; Jeong, S. Y., Extremely Efficient Liquid Exfoliation and Dispersion of Layered Materials by Unusual Acoustic Cavitation. Sci. Rep. **2014**, *4*.